JACS
JOURNAL OF THE AMERICAN CHEMICAL SOCIETY

ARTICLE

pubs.acs.org/JACS

Positive and Negative Design Leads to Compositional Control in AAB Collagen Heterotrimers

Lesley E. R. O'Leary, Jorge A. Fallas, and Jeffrey D. Hartgerink*

Department of Chemistry and Department of Bioengineering, Rice University, 6100 Main Street, Mail Stop 602, Houston, Texas 77005, United States

Supporting Information

ABSTRACT: Although collagen is the most abundant protein in the human body and has at least 28 types, research involving collagen mimetic systems only recently began to consider the innate ability of collagen to control helix composition and register. Collagen triple helices can be homotrimeric or heterotrimeric, and while some types of natural collagen form only one specific composition of helix, others can form multiple compositions. It is critical to fully understand and, if possible, reproduce the control that native collagen has on helix composition and register. In this Article, we utilize both positive and negative design for the assembly of specific AAB heterotrimers using charged amino acids to form intrahelix electrostatic interactions, which promote heterotrimer formation and simultaneously discourage homotrimers. Homotrimers are further discouraged by reducing hydroxyproline content, which would otherwise lead to nonspecific promotion of triple helix formation. We combine peptides in a 2:1 ratio in which the more abundant peptide has a charge 1/2 and opposite of the less abundant peptide, which can result in the formation of a zwitterionically neutral AAB heterotrimer. Using this approach, we are able to design collagen mimetic systems with full control over the composition of the resulting triple helix. All previous reports on synthetic collagen heterotrimers have shown mixed populations with respect to composition due to varying amounts of residual homotrimers. Our results yield a greater understanding of the self-assembly of collagenous sequences as well as provide a novel design scheme, both positive and negative, for the synthesis of extracellular matrix mimetics.

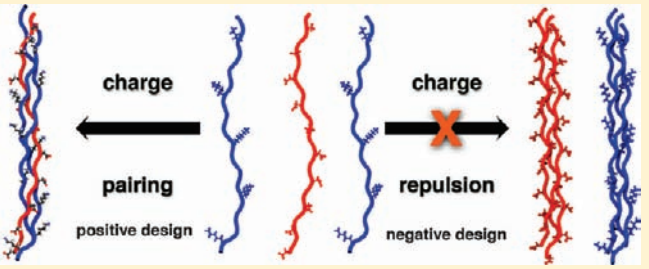

INTRODUCTION

Although collagen is the most abundant protein in the human body and has been studied for decades, the ability of mimetic systems to replicate the control of helix composition and register has only recently been considered.[1] There are 28 known types of collagen that can form homotrimeric (AAA) or heterotrimeric (AAB and ABC) compositions. While some types, such as collagen type I, form one composition of helix (in this case an AAB heterotrimer), others such as type V can form both AAB and ABC heterotrimers.[2] The control that native collagen has on helix composition and register, especially for collagen types that can form multiple types of triple helices, is a subject that is not well understood and has yet to be reproduced by collagen mimetic peptides, but one that is critical for replicating the structure and properties of this protein.

The amino acid sequence of natural collagen has a distinct repeating pattern Xxx−Yyy−Gly, where the X position is most commonly proline (Pro = P) and the Y position is predominantly hydroxyproline (Hyp = O), an amino acid that is post-translationally modified from proline by the addition of a hydroxyl group on the γ-carbon.[1,3] Because of this unique amino acid pattern, mimics of collagen are frequently examined using the triplet Pro−Hyp−Gly (POG in single letter code) as a template. Using collagen mimetics based on $(POG)_n$, studies on the folding kinetics,[4] amino acid propensities,[3,5,6] helical twist,[7] and stabilizing forces of triple helices[8] have been performed. In addition, the repeating triplet of collagen drives the staggered assembly of peptides within helices such that the second peptide is offset from the first by one amino acid and the third is offset by two amino acids. This staggering allows for glycine residues to inhabit the center of the triple helix throughout its length as well as dictates unique peptide registers that can be present in heterotrimeric systems: specifically, an AAB heterotrimer can have three different registers (AAB, ABA, or BAA) depending on which peptides are in the leading, middle, and lagging strands, respectively.

For over a decade, research has focused on the formation of collagen mimetic triple helices: first as homotrimers and, more recently, as heterotrimers. Many different strategies for the formation of these systems have been used including the incorporation of natural collagen sequences,[9] electrostatic interactions,[10−14] hydrophobic interactions,[3,15] cysteine knots,[16] and amino acid propensity.[3,5,6,14] These approaches have utilized a positive design stratagem in which moieties are incorporated into the peptide design to induce a certain outcome. The

Received: December 13, 2010
Published: March 23, 2011

dx.doi.org/10.1021/ja111239r | J. Am. Chem. Soc. 2011, 133, 5432–5443

majority of collagen mimetic research has been on homotrimeric species, and, although this research has greatly enriched knowledge within the field, the ability of these systems to accurately replicate heterotrimeric collagen such as types I, IV, and VIII is limited. To study diseases that affect these collagen types, for example Osteogenesis Imperfecta and Ethers-Danlos syndrome, which can result from a single mutation in only one or two of the peptide strands within the triple helix,[17] a collagen mimetic system that selectively forms a heterotrimer of a single register is needed.

In 2007, we reported a design for the formation of high stability ABC heterotrimers, which utilized the combination of an electrostatically positive peptide (charge = $+n$), an electrostatically negative peptide (charge = $-n$), and a neutral peptide in a 1:1:1 ratio to drive the formation of the triple helix.[11,12] In 2009, the ABC heterotrimer with the highest melting temperature from this study was further analyzed using 2D solution NMR experiments and was found to form a single register with $(PKG)_{10}$ as the leading strand, $(DOG)_{10}$ as the middle chain, and $(POG)_{10}$ as the lagging peptide.[10] Although these results established the first system to selectively form an ABC heterotrimer, a major drawback of the system is the ability of the $(POG)_{10}$ peptide to form a high stability homotrimer. The formation of this homotrimer makes the assembly of the heterotrimer more difficult by requiring a thermal annealing step, and, generally, the competition between this species and the desired product reduces the homogeneity of heterotrimer solutions. In a designed system in which homotrimer formation is discouraged, the desired heterotrimer would be the most stable triple helix within the system, maximizing its population. Furthermore, in an ideal system, none of the peptides would be able to form stable homotrimers, and only the desired heterotrimer could fold.

Recently, we reported the formation of a high stability AAB heterotrimer driven by electrostatic interactions whose major component was of a single peptide register.[18] Although this result was not the first published system to form this type of triple helix,[9] the novel aspect of the 2010 paper was that the reported heterotrimer, formed by the 2:1 mixture of $(EOGPOG)_5$ and $(PRG)_{10}$ where E is glutamic acid and R is arginine, had a thermal stability higher than the homotrimer of either peptide, and 2D solution NMR confirmed that the major component within the system was of a single register: $(PRG)_{10}\cdot(EOGPOG)_5\cdot(EOGPOG)_5$.[18] The greater stability of the ABB heterotrimer over either possible homotrimers was the result of effective interpeptide charge screening coupled with reduction of the total number of POG triplets (which are strong stabilizers of homotrimeric helices) within any peptide and charge repulsion within either possible homotrimer. The combination of charge−charge repulsion and reduction of POG triplet reduced the thermal stability of the negatively charged peptide by 21 °C and entirely eliminated the formation of homotrimers from the positively charged peptide. Since this publication, two more AAB triple helix forming systems have been reported that form AAB heterotrimers by utilizing a tethering technique to covalently link peptide chains together and drive heterotrimer formation[19] and a computational approach to design low-stability collagen heterotrimers by maximizing interactions between arginine and glutamic acid and eliminating POG-repeats within the peptides.[20]

In this Article, we further explore our design for AAB heterotrimer formation by considering peptides designed with lysine (K) and aspartic acid (D). This allows us to examine triple helices with R−D-, R−E-, K−D- and K−E-based salt bridges. Using the same charge ratios as described above, we utilize both positive and negative design in our peptide systems through the incorporation of charged amino acids to form electrostatic interactions promoting heterotrimer formation and by the placement of the charged residues within POG-containing peptides to discourage homotrimer formation. A total of eight peptide chains are examined (see Table 1). Among the triple helices studied, $2(PKGPOG)_5\cdot(EOG)_{10}$ and $2(PKGPOG)_5\cdot(DOG)_{10}$ are the first reported heterotrimeric collagen systems to form heterotrimers, while none of the component POG-containing peptides form homotrimers, demonstrating the success of the negative design aspect of this method for AAB heterotrimer formation. The 2D solution NMR results on these peptide systems prove that, for the first time, a heterotrimeric system is reported in which there is control over heterotrimer composition such that all species within the system are of a single composition. All previous reports on high-stability heterotrimeric systems utilized peptides that formed homotrimers of various quantities. Therefore, despite heterotrimer formation, a small population of homotrimer was always present. We also observe that the arginine−aspartic acid charge pair cannot form a heterotrimer. We believe that this is due to the interaction between the arginine side chain with a backbone carbonyl, which prevents the arginine from adopting the conformation necessary to optimally hydrogen bond with aspartic acid. In contrast, all systems containing the combination of lysine and aspartic acid formed heterotrimers, which suggests the possibility of a direct interaction between the charged residues similar to previous reports on an ABC heterotrimer.[10] Finally, the composition and ionic strength of examined buffer systems were found to play a large role in determining heterotrimer stability in systems where homotrimers were also present. Together, our results provide a novel design scheme for synthetic extracellular matrix mimetics as well as a better understanding of the self-assembly of collagenous sequences.

Table 1. Peptide Library and T_m of Corresponding Homotrimer Formation As Determined by CD

peptide	phosphate	Tris	Tris/NaCl
$(PRG)_{10}$	none	none	37 °C
$(PKG)_{10}$	none	none	none
$(EOG)_{10}$	none	none	none
$(DOG)_{10}$	none	39.5 °C	37.5 °C
$(PRGPOG)_5$	55.5 °C	56 °C	56.5 °C
$(PKGPOG)_5$	none	none	none
$(POGEOG)_5$	43 °C	43 °C	43.5 °C
$(POGDOG)_5$	35.5 °C	33 °C	35.5 °C

EXPERIMENTAL SECTION

Peptide Synthesis and Purification. All peptides were synthesized on an Advanced Chemtech Apex 396 multipeptide automated synthesizer using standard Fmoc chemistry for solid-phase peptide synthesis. Rink Amide MHBA resin was used for all peptides, and the synthesis was performed at a 0.15 mM scale. Purification was performed on a Varian PrepStar220 HPLC using a preparative reverse phase C-18 column. Purified peptides were analyzed either by MALDI/TOF mass spectrometry on a Bruker Autoflex II or by ESI/TOF mass

spectrometry on a Bruker microTOF. Peptides $(PRG)_{10}$, $(PKG)_{10}$, $(EOG)_{10}$, and $(DOG)_{10}$ were previously synthesized and reported.[11,12,18] Peptides $(PKGPOG)_5$, $(POGDOG)_5$, $(POGEOG)_5$, $WG(PKGPOG)_5$, $WG(EOG)_{10}$, and $WG(DOG)_{10}$ were newly prepared for this study. HPLC chromatograms and mass spectra for the newly synthesized peptides are given in the Supporting Information.

Circular Dichroism. All CD experiments were performed with a Jasco J-810 spectropolarimeter equipped with a Peltier temperature control system using quartz cells with a path length of 0.1 cm. Samples were heated to 85 °C for 15 min and subsequently incubated at 10 °C overnight before spectra and melting experiments were performed. Spectra were taken from 190 to 250 nm, and the wavelength of the maximum seen in the spectra, between 223 and 225 nm, was monitored during thermal unfolding curves. Melting experiments were performed from 5 to 85 °C with a temperature increase of 10 °C/h. The first derivative of the melting curve was taken to determine the melting temperature (T_m) of the sample. The molar residual ellipticity (MRE) is calculated from the measured ellipticity using the equation:

$$[\theta] = \frac{\theta \times m}{c \times l \times n_r}$$

where θ is the ellipticity in mdeg, m is the molecular weight in g/mol, c is the concentration in mg/mL, l is the path length of the cuvette in cm, and n_r is the number of amino acids in the peptide.

Differential Scanning Calorimetry. All DSC experiments were performed on a VP-DSC MicroCalorimeter from MicroCal using the same temperature parameters as the CD experiments (range of 5−85 °C with a scan rate of 10 °C/h). After reaching the maximum temperature, the sample was rapidly cooled to 5 °C and equilibrated at that temperature for 1 h before beginning the next scan. All samples were dialyzed for 3 days in buffer prior to each experiment. The DSC curves of the dialysis buffer were used as the baseline and subtracted from each peptide curve prior to data analysis. Heat capacity (C_p) baseline before and after unfolding was also subtracted, resulting in a baseline value of zero. During data analysis, the curves were normalized to the triple helix concentration by dividing the measured total peptide concentration (determined by mass) by 3. The melting temperature of the system was defined as the temperature at which the maximum measured C_p was observed.

Nuclear Magnetic Resonance. NMR samples were prepared in a 9:1 ratio of H_2O to D_2O at pH 7. Peptides were mixed in a 2:1 ratio to a total concentration of 3.6 mM, determined by tryptophan absorption at 280 nm. The $2WG(PKGPOG)_5 \cdot WG(DOG)_{10}$ mixture was prepared in 10 mM phosphate buffer, and the $2WG(PKGPOG)_5 \cdot WG(EOG)_{10}$ was in 10 mM deuterated Tris (tris(hydroxymethyl)-aminomethane) buffer. The $WG(PKGPOG)_5$ contains a single ^{15}N-labeled glycine (amino acid 20), purchased from isotech, in the sixth triplet.

All NMR experiments were recorded in a 600 MHz Varian Inova spectrometer unless otherwise noted, processed using the NMRpipe software and analyzed using Sparky. Both systems were characterized using homonuclear $^1H,^1H$-NOESY and $^1H,^1H$-TOCSY experiments. Also, $^1H,^{15}N$-sofast-HMQC[21] spectra were acquired without ^{15}N decoupling and with a 1 s acquisition time. The in-phase and antiphase spectra were combined and shifted by $1/2\ J_{NH}$ in opposite directions to reconstruct the nonsplit spectra as described by Brutscher et al.[21] Furthermore, $^1H,^1H$-planes of a 3D HNHA and NOESY-^{15}N-HSQC were recorded for each sample by keeping the chemical shift evolution constant in the heteronuclear dimension. For ease of discussion, we will refer to the HNHA experiment as a 2D HNHA and the NOESY-^{15}N-HSQC as an edited NOESY spectrum. The latter was acquired on an 800 MHz Varian spectrometer. All acquisition and processing parameters are available in the Supporting Information.

RESULTS AND DISCUSSION

As previously mentioned, the design for heterotrimer formation is based on combining peptides in a 2:1 ratio in which the more abundant peptide has a charge 1/2 and opposite of the other, allowing for the possibility of forming a zwitterionic, neutral AAB heterotrimer. Its formation is driven by the combination of the positive design motif in which we provide electrostatic interactions between the oppositely charged amino acids and the negative design strategy in which we discourage homotrimer formation by charge repulsion and a reduction of the number of POG repeats present in each peptide.

As with all previously reported heterotrimeric systems, the ability of all peptides within the library to form homotrimers must be understood before the mixture of peptides can be pursued.

CD on Homotrimers. The entire peptide library explored is given in Table 1 as well as the homotrimer melting temperatures of each in the three buffers examined: 10 mM phosphate, 10 mM tris(hydroxymethyl)-aminomethane (Tris), and 10 mM Tris 150 mM sodium chloride (NaCl), all at pH 7. Detailed melting profiles for all peptides are given in the Supporting Information. Previously, we primarily used phosphate buffers in systems for heterotrimer formation. However, recently we began exploring the differences in homotrimer and heterotrimer stabilities in different buffer systems as we observed that in some instances they can be highly dependent both on buffer composition and on overall ionic strength as would be expected for systems whose assembly is highly dependent on charge pair interactions. More specifically, we investigated phosphate versus Tris and how the addition of NaCl to increase the ionic strength would affect melting temperatures. In terms of peptide design for homotrimer formation, we are interested in discouraging homotrimer formation as much as possible by implementing a negative design technique. In general, for collagen mimetic systems, the more POG repeats that are present in a peptide chain, the more likely it will be to form a homotrimer. It is for this reason that we do not expect ±10 charged peptides to form homotrimers, but are not surprised when ±5 charged peptides assemble into homotrimeric helices. When examining Table 1, two observations can be made: (1) $(PRG)_{10}$ and $(DOG)_{10}$ do in fact form homotrimers in at least one of the buffer systems despite the putative charge repulsion preventing such assembly, and (2) $(PKGPOG)_5$ does not form a homotrimer in any buffer system tested despite the presence of five POG triplets within the peptide and having just 1/2 the charge of the above peptides.

On the basis of the previous results, we did not expect for any of the peptides with ±10 charges to form homotrimers in any of the low ionic strength buffers. In the presence of high ionic strength buffers, host−guest peptides containing one or more PRG triplets had been previously shown to form a homotrimer in PBS (10 mM phosphate with 150 mM NaCl), pH 7, and, in the same study, $(PRG)_8$ formed a homotrimer in 10 mM sodium phosphate, 2 M NaCl, pH 7.[22] Complementing those studies, we found that $(PRG)_{10}$ forms a homotrimer with a T_m of 37 °C in Tris/NaCl, another high ionic strength buffer. In recently reported DSC experiments on $(PRG)_{10}$, a small population of peptide formed a homotrimer in 10 mM phosphate buffer.[18] We hypothesize that the guanadinium within the side chain of arginine interacts with a backbone carbonyl of hydroxyproline in an adjacent strand stabilizing the homotrimer. This interaction is masked by charge repulsion in low ionic strength buffers.

Table 2. Peptide Mixtures and CD Melting Transitions

peptide mixture	T_m in phosphate	T_m in Tris	T_m in Tris/NaCl
$(PRG)_{10}\cdot 2(POGDOG)_5$	mult pks	mult pks	overlap
$2(PRGPOG)_5\cdot (DOG)_{10}$	mult pks	mult pks	mult pks
$(PRG)_{10}\cdot 2(POGEOG)_5$	47 °C	51.5 °C	overlap
$2(PRGPOG)_5\cdot (EOG)_{10}$	52.5 °C	53 °C	47 °C
$(PKG)_{10}\cdot 2(POGDOG)_5$	44 °C	48 °C	43 °C
$2(PKGPOG)_5\cdot (DOG)_{10}$	46 °C[a]	48 °C	43 °C
$(PKG)_{10}\cdot 2(POGEOG)_5$	40 °C	overlap	39 °C
$2(PKGPOG)_5\cdot (EOG)_{10}$	45 °C[a]	45 °C[a]	42 °C[a]

[a] Heterotrimer formation when neither of the component peptides forms homotrimers.

However, in PBS and Tris/NaCl, the arginine side chain charges are sufficiently screened by the high salt concentration allowing for the majority of the peptide population to form stable homotrimers. The more surprising result within the homotrimer study on ±10 charged peptides is that $(DOG)_{10}$ forms a homotrimer in both Tris and Tris/NaCl buffers. We hypothesize that the cationic nature of the Tris buffer might allow for a specific stabilizing interaction (as opposed to simple charge screening) between Tris and the negatively charged aspartic acid, preventing side chain charge repulsion and allowing for triple helix formation in the lower ionic strength buffer. This interaction is then weakened with the addition of NaCl to the buffer, which decreases the thermal stability, lowering the melting temperature of the homotrimer by 2 °C.

The second observation, and arguably the most notable result within this table, is the inability of $(PKGPOG)_5$ to form a homotrimer in any of the three buffers formed. On the basis of the 2007 studies by our lab,[11,12] peptides with ±5 charges are expected to fold in phosphate buffer with T_m values between 30 and 40 °C. One possible explanation for the current observation is based on the amino acid propensity for forming stable collagen triple helices, which have shown that lysine in the Y-position of a collagen triplet has a far lower stability than arginine, causing it to have a lower propensity for triple helical formation.[6] From the perspective of negative design in which the formation of unwanted species within a system is discouraged, the inability of this peptide to form a stable homotrimer makes it unique within the library as the lone peptide that, when combined with a −10 charged peptide, could potentially form an AAB heterotrimer in the absence of either peptide forming a homotrimer.

CD on Heterotrimers. On the basis of the previously described peptide design, oppositely charged peptides were mixed in a 2:1 ratio to generate zwitterion AAB triple helices. All peptide mixtures and the transitions seen in CD melting studies in all three buffers are listed in Table 2 and are organized on the basis of the charged residues present in the pairing: R−D, R−E, K−D, and K−E. If the unfolding transition seen in mixtures overlapped any homotrimer transitions within the range of ±2 °C, "overlap" is written in the table. If the transition did not overlap, the melting temperature is listed. Last, if multiple transitions were seen in CD melting studies indicating the inability of a specific system to form a clean AAB heterotrimer, "mult pks" is listed in the table.

There are three major points to discuss before an in-depth analysis of each charge pairing progresses. First, all of the peptide mixtures examined that form heterotrimers have their highest melting temperatures in Tris buffer, reiterating the ideas proposed during the homotrimer discussion that Tris has a stabilizing effect on negatively charged peptides. Second, the direct comparison of results in Tris versus Tris/NaCl exposes the charge shielding that results from a higher ionic strength buffer, which, depending on the system, either hid or unveiled the presence of an AAB heterotrimer by altering the relative thermal stability of homo- versus heterotrimers. This characteristic demonstrates the versatility of the design system for AAB heterotrimer formation and the challenges associated with it because by adjusting the ionic strength of the buffer used, visible heterotrimers unfolding transitions can be seen for three out of the four amino acid pairings examined in the proper buffer composition. Third, the ability of two of the peptide systems to form heterotrimers when none of the component peptides form homotrimers strongly suggests that we have compositional control over triple helix assembly based on the CD melting studies. This point can only be hypothesized on the basis of the CD melting studies, but is confirmed using 2D solution NMR experiments (below), making this the first reported heterotrimeric system in which there is complete control over heterotrimer composition.

Beginning with the arginine−aspartic acid pairing, $(PRG)_{10}\cdot 2(POGDOG)_5$ and $2(PRGPOG)_5\cdot (DOG)_{10}$, it is immediately apparent from the table that neither of the two systems examined using the combination of these residues forms a clean heterotrimer: multiple peaks are seen in all peptide mixtures. Figure 1 gives an example of these results from the $2(PRGPOG)_5\cdot (DOG)_{10}$ system in Tris buffer. All remaining mixtures within this charge pairing are given in the Supporting Information. To understand these results, we turn to our hypothesis for homotrimer stabilization in PRG-containing peptides: the interaction between the guanadinium in the arginine side chain with the backbone carbonyl of hydroxyproline in an adjacent strand. For heterotrimer formation with these peptides, we believe that this interaction is still present, which prevents the arginine terminal amines from forming a salt bridge with the carboxyl group on aspartic acid.[12] It is for this reason that, even if a heterotrimer peak is seen in mixtures of arginine- and aspartic acid-containing peptides, homotrimer peaks can still be seen. This has a deleterious effect on both positive and negative design: the desired heterotrimer is destabilized as optimal conformations allowing arginine−aspartic acid interactions are prevented while simultaneously stabilizing unwanted homotrimers through arginine−backbone hydrogen bonding.

When we consider the arginine−glutamic acid pairing, a drastic difference can be seen when compared to the arginine−aspartic acid coupling: heterotrimer formation can be seen in at least one buffer for both systems. This complements the results published earlier this year that the mixture of $(PRG)_{10}\cdot 2(EOGPOG)_5$ forms a stable heterotrimer in Tris buffer.[18] We attribute the previous result and those for our two new systems to the fact that glutamic acid has one more methylene group than aspartic acid, which allows for closer interaction between the oppositely charged amino acids and therefore better shielding of side chain charges while still maintaining the hydrogen bond between the guanidinium group of arginine and the hydroxyproline backbone carbonyl. The final item that must be noted within this charge pairing is the lack of clear heterotrimer formation for the $(PRG)_{10}\cdot 2(POGEOG)_5$ system in Tris/NaCl. The increase in ionic strength destabilized the nonspecific charge interaction between the arginine and glutamic acid residues, causing a

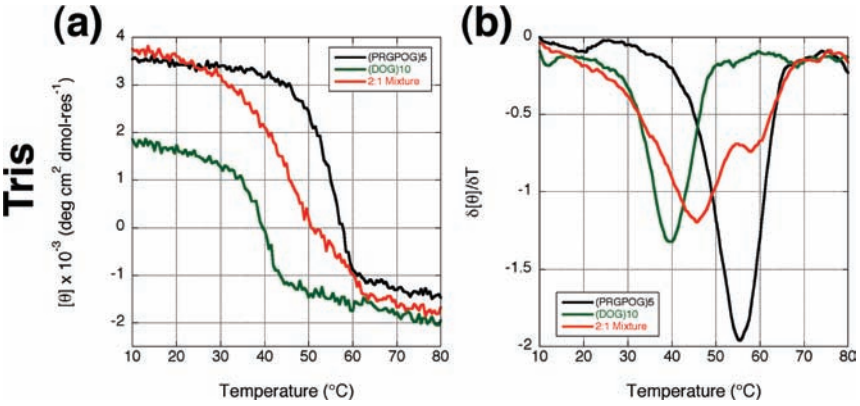

Figure 1. Circular dichroism thermal unfolding curves for $(PRGPOG)_5$ (black), $(DOG)_{10}$ (green), and the 2:1 mixture of $(PRGPOG)_5$ and $(DOG)_{10}$ (red) in Tris shown as (a) MRE versus temperature and (b) first derivative of MRE versus temperature.

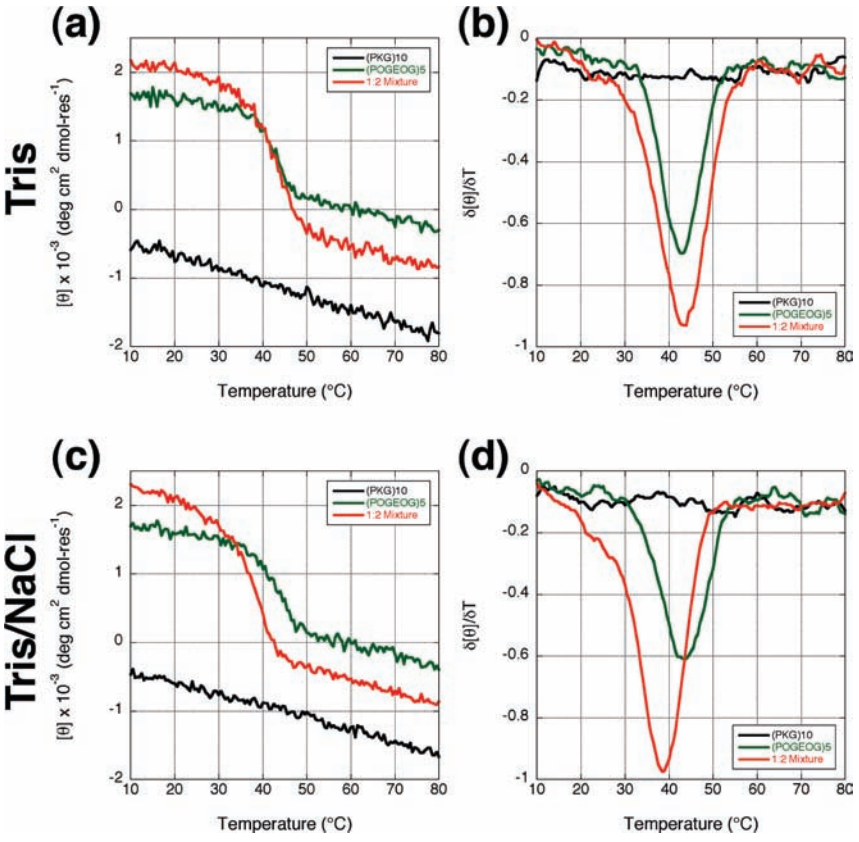

Figure 2. Circular dichorism thermal unfolding curves for $(PKG)_{10}$ (black), $(POGEOG)_5$ (green), and the 1:2 mixture of $(PKG)_{10}$ and $(POGEOG)_5$ (red) in Tris (a and b) and Tris/NaCl (c and d). The graphs are shown as MRE versus temperature (a and c) and first derivative of MRE versus temperature (b and d).

decrease in the melting temperature of the triple helix, making it comparable to the T_m for the $(POGEOG)_5$ homotrimer. This masking and unveiling of heterotrimer formation based on the ionic strength of buffers will be discussed further below. The melting curves for both systems in all three buffers are all given in the Supporting Information.

Moving to peptide mixtures containing lysine residues, the pairing of lysine and glutamic acid will be discussed first. Similar to the results with arginine and glutamic acid, both peptide systems form a distinct heterotrimer in at least one buffer. $(PKG)_{10}\cdot 2(POGEOG)_5$ results in a heterotrimer with a lower stability than the homotrimer in phosphate (not shown). In Tris (shown in Figure 2a and b), heterotrimer formation is masked by the overlapping T_m between the peak of the peptide mixture and the $(POGEOG)_5$ homotrimer. Upon the addition of NaCl (Figure 2c and d), the heterotrimer peak becomes visible with a T_m of 39 °C, which is lower than the homotrimer, demonstrating the heterotrimer unmasking that can occur by adjusting the ionic strength of the buffer. Results for this peptide system in phosphate are given in the Supporting Information. When we

dx.doi.org/10.1021/ja111239r |*J. Am. Chem. Soc.* 2011, 133, 5432–5443

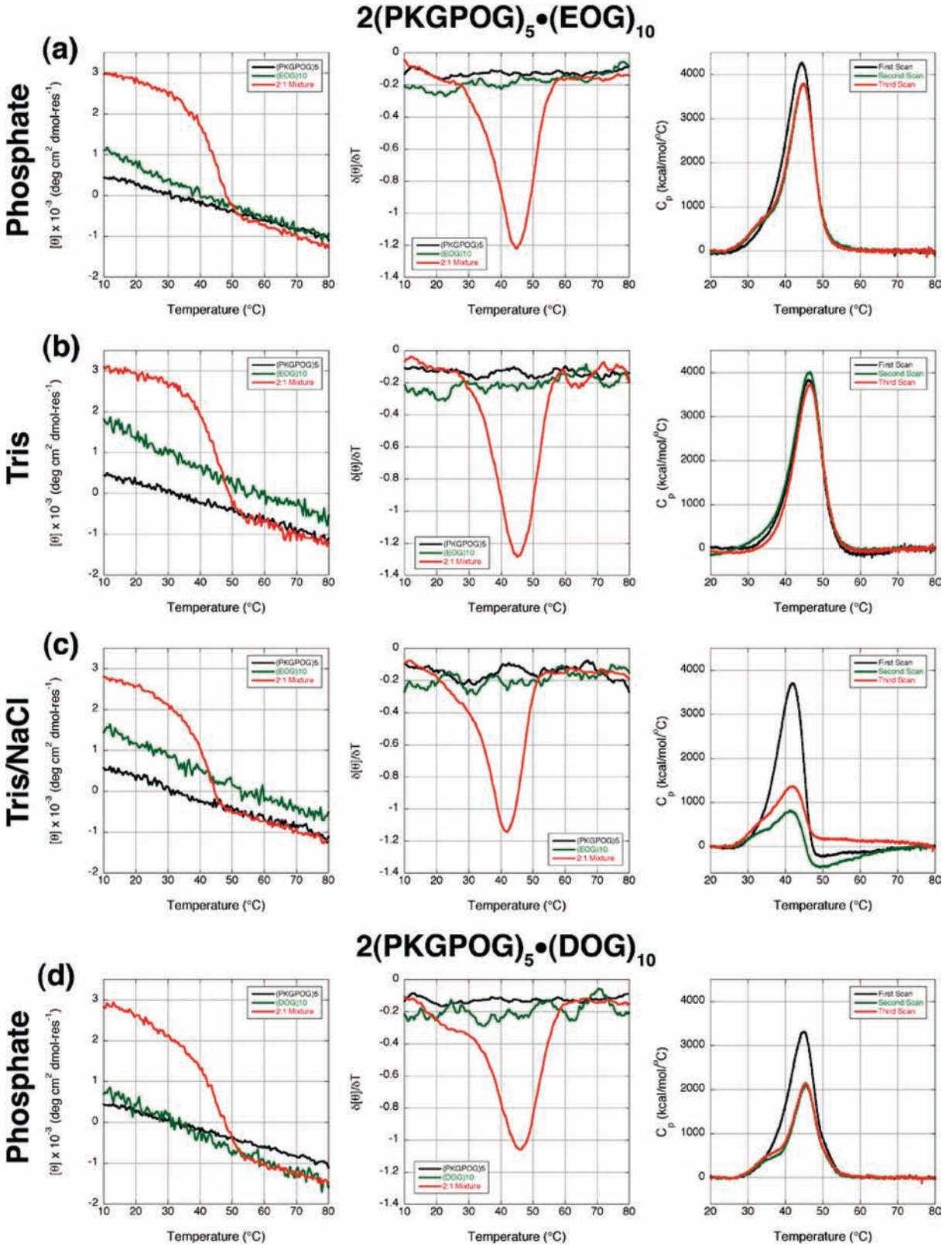

Figure 3. Circular dichorism thermal unfolding curves (left and center columns) and differential scanning calorimetry melting profiles (right column) for $2(PKGPOG)_5 \cdot (EOG)_{10}$ in (a) phosphate, (b) Tris, (c) Tris/NaCl, and $2(PKGPOG)_5 \cdot (DOG)_{10}$ in (d) phosphate. The melting profiles for each system are given as MRE versus temperature in the left column and the first derivation of MRE versus temperature in the center column with data for the component peptides shown in black and green and the data for the mixture of the two peptides given in red.

invert the charge pair going from +10/−5 to +5/−10 with $2(PKGPOG)_5 \cdot (EOG)_{10}$, a heterotrimer is formed in all samples (T_m of 45 °C in phosphate and Tris and T_m of 42 °C in Tris/NaCl), while none of the two individual peptides form homotrimers

dx.doi.org/10.1021/ja111239r |*J. Am. Chem. Soc.* 2011, 133, 5432–5443

in any of the three buffers. This high-stability AAB triple helix formation when neither of the component peptides forms a homotrimer helix demonstrates the successful implementation of both positive and negative design parameters. Previously, Xu et al. also demonstrated the formation of an AAB type triple helix in which neither of the component peptides formed homotrimers.[20] It is worth noting that in Xu's system the peptides contain zero POG triplets and are also not charge neutral. While the lack of POG triplets reduces chance of homotrimer formation, it also decreases the thermal stability of the AAB systems formed (for example, they report at T_m of 20 and 22 °C as compared to 45 and 46 °C here). In our system, due to the fact that neither peptide forms a homotrimer, any triple helix seen in 2:1 mixtures of the peptides must result from stabilizing interactions between peptides upon heterotrimer formation. These interactions are most likely between lysine and glutamic acid as will be shown below by NMR. The melting profile and first derivative for this system in all of three buffers are given in Figure 3a−c (phosphate, Tris, and Tris/NaCl, respectively). Because this system results in heterotrimers without homotrimer formation in all three buffers, we continued analysis of all $2(PKGPOG)_5 \cdot (EOG)_{10}$ mixtures by performing DSC experiments. These results are shown in the right column of Figure 3a−c, respectively, and are described below.

The last amino acid pair that we analyzed is the combination of lysine and aspartic acid, which had previously been shown to form direct electrostatic interactions within a self-assembled ABC heterotrimer.[10] The first major observation about the results on $(PKG)_{10} \cdot 2(POGDOG)_5$ and $2(PKGPOG)_5 \cdot (DOG)_{10}$ is the presence of thermal transitions for AAB heterotrimers in all buffers regardless of the charge combination being +10/−5 or +5/−10. This makes the lysine−aspartic acid charge pairing different from, and superior to, the other three charge combinations tested. In addition, all of the heterotrimers observed have higher thermal stabilities than any homotrimer in the systems. Again, this is the only amino acid pairing with such results. Before discussing the possible driving forces for this heterotrimeric stability, a second observation must be made. In all three buffers, the melting temperatures between the systems are within two degrees of each other even though the stabilities of the homotrimers are varied significantly. We hypothesize that there is direct electrostatic bridging between the lysine and aspartic acid residues, which is possible with lysine−aspartic acid pairing as opposed to the previously discussed arginine−aspartic acid combinations due to the structural freedom of the lysine side chain. This direct salt bridge was previously reported on an ABC system and was shown to occur between lysines of triplet *n* and aspartic acids of triplet $n + 1$.[10] However, in both AAB mixtures, only five bridges would be possible based on the peptide design. To confirm this theory, further analysis using DSC and 2D solution NMR was required. For such analysis, we selected the $2(PKGPOG)_5 \cdot (DOG)_{10}$ system in phosphate due to the fact that it forms an AAB heterotrimer without either component peptide forming a homotrimer, allowing for cleaner analysis and again demonstrating the successful implementation of positive and negative design strategies to achieve a desired result. The CD melting profile for $2(PKGPOG)_5 \cdot (DOG)_{10}$ in phosphate is shown in Figure 3d. CD melting profiles for $2(PKGPOG)_5 \cdot (DOG)_{10}$ in Tris and Tris/NaCl as well as for $(PKG)_{10} \cdot 2(POGDOG)_5$ in all three buffers are given in the Supporting Information.

DSC on Selected Systems. After CD melting experiments were performed on all amino acid charge pair combinations, two peptide systems were highlighted for DSC analysis: $2(PKGPOG)_5 \cdot (EOG)_{10}$ in phosphate, Tris and Tris/NaCl and $2(PKGPOG)_5 \cdot (DOG)_{10}$ in phosphate. The profiles for each of these systems are shown in the right column of Figure 3a−d, respectively. To begin with, the melting temperatures seen in the first peptide scan for all samples matched the T_m seen in CD melting studies and are given in Table 2. The DSC melting experiments for each system give an alternative and more sensitive measure of the melting temperature, which confirms results from CD. Additionally, DSC gives us information about the thermal recovery, or lack thereof, for each heterotrimer. If we look at $2(PKGPOG)_5 \cdot (EOG)_{10}$ first, there are strong contrasts in the DSC melting profiles in each of the three buffers. In the right column of Figure 3a, the peptide system in phosphate shows a clean single peak in the first peptide scan; however, in the second and third scans, a shoulder at 30 °C can be seen. Because neither peptide forms a homotrimer visible by CD or DSC experiments, on the basis of these DSC results alone, we hypothesize that a kinetically trapped AAB heterotrimer may be forming in all subsequent melting scans. When the profile in phosphate is compared to that seen in Tris (right column of Figure 3a and b, respectively), a substantial difference can be seen. The profile in Tris shows a single transition in the first peptide scan that is repeated in all subsequent scans, indicating that any species present within the system refolds within the time scale of the experiment (at the beginning of each thermal scan, the system is allowed to equilibrate at 5 °C for 60 min). In the last buffer tested, Tris/NaCl shown in the right column of Figure 3c, a total breakdown of the AAB heterotrimer occurs after the first thermal scan. The second scan has a large shoulder at 30 °C, and the major peak has a much lower intensity that continues to decrease in the third scan. Although this result is disappointing for the thermal recovery of the peptide system, it is not unexpected due to the high salt concentration of the buffer. In such an environment, the high salt is expected to largely prevent the charged residues from forming significant interactions and thus slowing the refolding time of the peptide mixture, causing it to greatly exceed that of the DSC experiment, which results in the decrease of the AAB heterotrimer population with each subsequent scan. Refolding CD experiments of this peptide system in all three buffers were performed and complemented the DSC results (available in the Supporting Information).

When we examine the $2(PKGPOG)_5 \cdot (DOG)_{10}$ system in phosphate, DSC experiments are similar to those of the $2(PKGPOG)_5 \cdot (EOG)_{10}$ in phosphate. The first peptide scan is a clean single peak that corresponds to the T_m seen in CD melting studies. However, in all subsequent scans, a shoulder can be seen, and the intensity of the major peak decreases significantly. Analogous to the $2(PKGPOG)_5 \cdot (EOG)_{10}$ system, the second and third scans overlap each other, suggesting that the refolding time of the mixture greatly exceeds that of the DSC experiment such that a large portion of the system is able to refold within the time scale of the experiment.

Therefore, from DSC experiments, only the $2(PKGPOG)_5 \cdot (EOG)_{10}$ system in Tris buffer was capable of complete thermal recovery within the time scale of the experiments.

NMR on Selected Systems. To study the composition and supramolecular topology of the triple helical assemblies that give rise to the cooperative transitions in the CD and DSC spectra, a

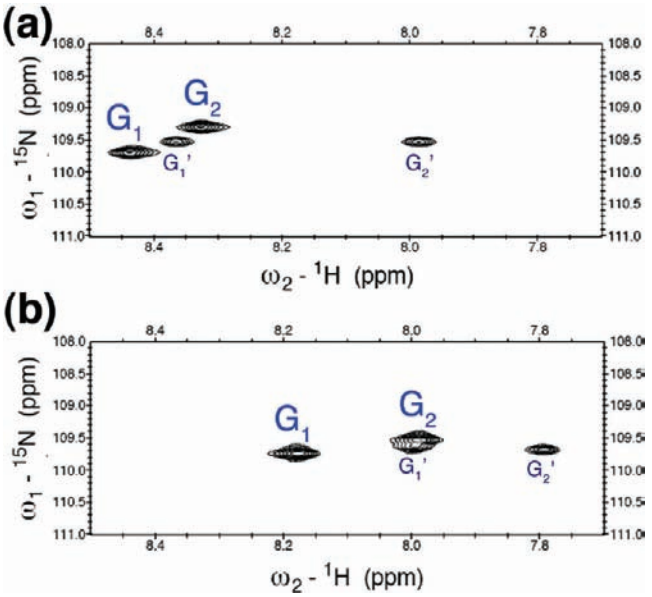

Figure 4. $^{1}H,^{15}N$-HMQC spectrum of (a) $2WG(PKGPOG)_5 \cdot WG(EOG)_{10}$ and (b) $2WG(PKGPOG)_5 \cdot WG(DOG)_{10}$. The cross peaks corresponding to the minor register are denoted by "′".

set of peptide derivatives of the $2(PKGPOG)_5 \cdot (DOG)_{10}$ and $2(PKGPOG)_5 \cdot (EOG)_{10}$ systems were synthesized. The derivatives include a tryptophan at the N-terminus of all peptides for accurate concentration determination and a glycine linker between the spectroscopic tag and the triple helical sequence. Furthermore, the sixth triplet of the $WG(PKGPOG)_5$ peptide contains an ^{15}N-enriched glycine (amino acid 20). Both systems were characterized using homonuclear $^{1}H,^{1}H$-NOESY and $^{1}H,^{1}H$-TOCSY experiments as well as $^{1}H,^{15}N$-HMQC and $^{1}H,^{1}H$-planes of 3D HNHA (2D HNHA) and NOESY-^{15}N-HSQC (edited NOESY). All experiments for the $2WG(PKGPOG)_5 \cdot WG(DOG)_{10}$ system were carried out in 10 mM phosphate buffer, while the $2WG(PKGPOG)_5 \cdot WG(EOG)_{10}$ was studied in a 10 mM deuterated Tris solution, both at neutral pH. A detailed description of the spectra used in the analysis and sample preparation is described in the Experimental Section.

The $^{1}H,^{15}N$-HMQC spectrum for each system shows two pairs of cross-peaks of equal intensity (Figure 4). Because the ^{15}N-labeled amino acid is present in the peptide chain with the lower overall charge, and therefore twice in each triple helix, two distinct cross-peaks are expected for each register of the desired AAB triple helix because the chemical environment is, in principle, not identical for both chains with identical sequence in the heterotrimer. On the other hand, a homotrimer or an AAB heterotrimer of the opposite stoichiometry would give rise to a single cross-peak. The spectra obtained show that both the $2WG(PKGPOG)_5 \cdot WG(DOG)_{10}$ and the $2WG(PKGPOG)_5 \cdot WG(EOG)_{10}$ systems populate two distinct sets of chemical environments. Furthermore, each of those environments includes two labeled glycines with equivalent populations but distinct chemical shifts as we expect for an AAB heterotrimer comprised of two positive chains and a negative one. We believe that those two environments are best accounted for by two competing registers of the desired heterotrimer and that no triple helical assembly of a different composition is significantly populated. With these data, we can conclude that this is the first time that a self-assembled heterotrimeric triple helical system shows control over composition as was suggested by the CD melting studies. This means that within this peptide mixture no competing homotrimers or alternative composition of heterotrimers are formed. Despite having control over the composition of the helix, the self-assembled AAB triple helices lack complete control over their register. The relative population of each register can be obtained by comparing the cross-peak intensity in the spectra. The integration leads to a 2.6:1 ratio between the major and minor registers for $2WG(PKGPOG)_5 \cdot WG(EOG)_{10}$ (72% of the triple helical population corresponds to the major register and 28% to the minor register). A similar result is obtained for the $2WG(PKGPOG)_5 \cdot WG(DOG)_{10}$ system where the ratio stands at 2.2:1 (69% of the triple helical population corresponds to the major register and 31% to the minor register).

The NOESY and TOCSY spectra of each system show the structure expected from a triple helical assembly. Because of the symmetry of the helix and the periodicity of the sequence, only one set of cross-peaks is observed for each amino acid in the structural repeating unit of each chain. In the case of the negative chain, the structure of the positive chain's sequence causes two consecutive triplets to be chemically distinct even though they are equivalent in sequence, making the repeating unit DOGDOG and EOGEOG instead of DOG and EOG, respectively. This differs from what has been previously observed for ABC heterotrimers,[10] where the repeating unit corresponds to a triplet, but agrees with our previous results for AAB heterotrimers, where the repeating unit corresponds to a sextet.[18] The backbone chemical shifts of the PKG triplet and EOGEOG and DOGDOG sextets were identified using the homonuclear sequential assignment procedure. For the POG triplets within the $WG(PKGPOG)_5$ peptide, a combination of the 2D HNHA and edited NOESY experiments was successful in identifying the glycine and hydroxyproline backbone chemical shifts, but the sequential following of two imino acids makes the identification of the proline H_α frequency for the POG triplets very difficult with the current experimental setup. Furthermore, no sequential links are available between the PKG and POG triplets that make up the repeating unit in the positive chains. NOEs between the glycines of these triplets were used to determine which chain each glycine belonged to. Because of constraints in the triple helical structure, no NOEs between the two consecutive glycines of the same chain are possible. Thus, NOEs between the glycines of PKG and POG triplets must be interchain and can be used to determine the chemical shift of the repeating units for the two chemically distinct positive chains. Because of spectral overlap in the aliphatic region, only a partial assignment of the amino acid's side chain resonances was possible, and the imino acid side chain assignment was not attempted.

Both the $^{1}H,^{1}H$-NOESY and the $^{1}H,^{1}H$-edited NOESY spectra show the cross-peaks expected from triple helical peptides. Such peaks include interchain proline delta to glycine amide correlations[23] as well as glycine amide−alpha and amide−amide resonances[10] due to the tight packing of glycines in the core of the helix. Other interesting features include resonances between lysine ε-protons and the acidic residue's amide proton, suggesting an interaction between the oppositely charged amino acids. This information, in principle, should suffice for

the determination of the register of the triple helices, but the task is complicated by the chemical shift overlap observed. In the next two sections, we discuss the distinctive features observed for each of the systems.

2WG(PKGPOG)$_5$·WG(EOG)$_{10}$. This system presents a particular challenge because the chemical shifts of the glutamic acid amide protons overlap with some of the glycines. Furthermore, some of the amide protons of the minor register overlap with the major register. For instance, the glycine amide proton chemical shift of the second EOG triplet in the major register overlaps with the glycine amide proton chemical shift of one of the POG triplets of the minor register. Thanks to the ^{15}N-label, this assignment can be made unambiguously. Yet in the regular NOESY spectrum, the cross-peaks corresponding to the minor register are obscured by those of the major register. In addition, the chemical shift of most of the glycine α-protons is degenerate. This leads to considerable spectral crowding of the region corresponding to the glycine amide−alpha proton resonances and makes the register determination impossible from this area. Instead, we focused on studying the relatively weak amide−amide resonances arising from glycine packing. In the regular NOESY spectrum, the area corresponding to the amide−amide cross-peaks is dominated by sequential and diagonal peaks. On the other hand, the edited NOESY spectrum provides a clear view of the region, and even though only information on the POG triplets can be gained, this provides enough information to determine the register. Figure 5a shows the edited NOESY spectrum for this system, where the chemical shifts of the labeled amino acids are marked by vertical lines and labeled as G_{O1} and G_{O2}. Each of those glycines presents cross-peaks to two other glycines, whose chemical shifts are marked by horizontal lines. From this information, we can deduce the register of the heterotrimeric triple helix. Starting at the G_{O1} chemical shift, two NOEs can be observed: one going to the glycine in the second triplet of EOGEOG repeating unit, labeled as G_{E2}, and one going to the PKG triplet in the second positive chain, labeled as G_{K2}. Now, considering the NOEs observed for G_{O2}, a cross peak to G_{E2} can also be observed, indicating that the second triplet of the negative chain is flanked by the two labeled glycines in the POG triplets of the positive chains, positioning it as the middle chain in the peptide register and making the register WG(PKGPOG)$_5$·WG(EOG)$_{10}$·WG(PKGPOG)$_5$. Figure 5b and c shows a sequence repeat to clarify the naming conventions used in the discussion and a heterotrimeric triple helix model. Furthermore, the observed NOEs between the glycine amide protons are highlighted in Figure 5c using colored arrows that match them to colored circles in Figure 5a. Most peaks from the minor register are below the level of noise, but a particular resonance between both POG triplets indicates that their glycines are in close proximity. A possible register that would agree with such an arrangement is WG(PKGPOG)$_5$·WG(PKGPOG)$_5$·WG(EOG)$_{10}$, which would be predicted on the basis of a recent theoretical paper

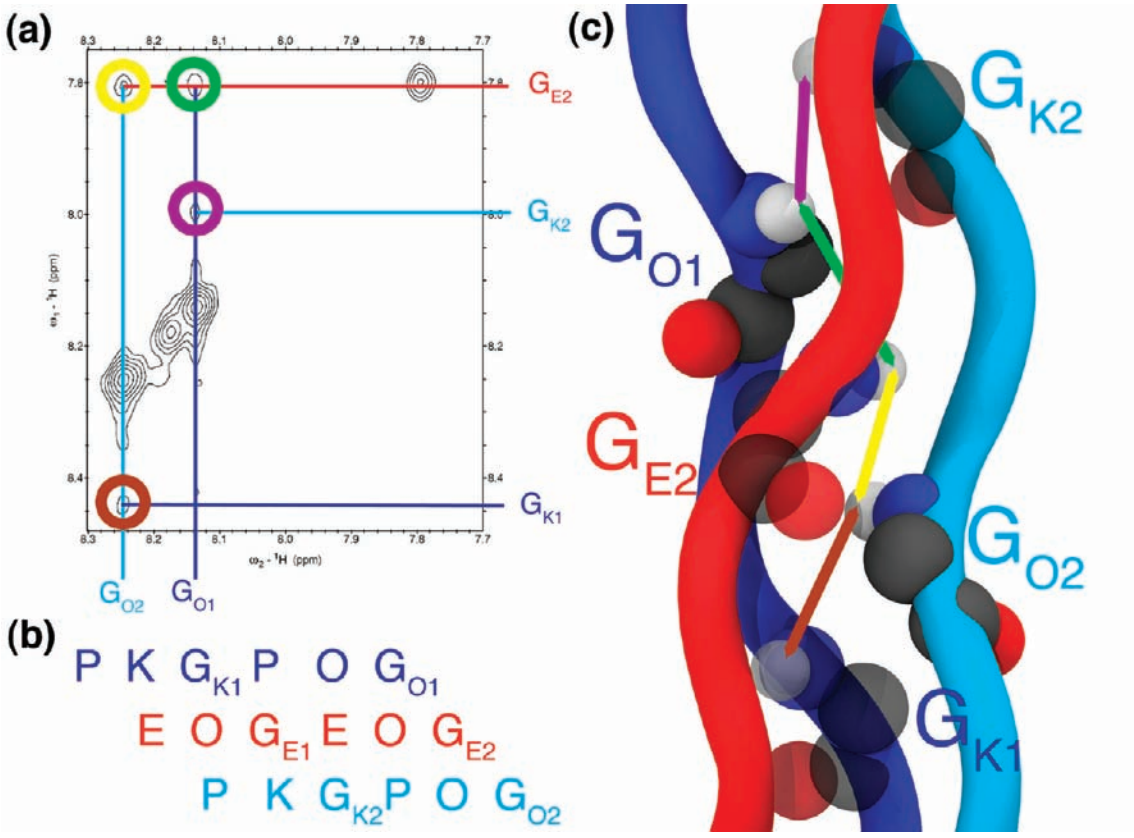

Figure 5. (a) ^{1}H,^{1}H-edited NOESY spectrum showing NH−NH resonances between chains, (b) molecular model highlighting the glycine packing interactions at the core of the helix, and (c) sextet repeat of WG(PKGPOG)$_5$·WG(EOG)$_{10}$·WG(PKGPOG)$_5$. In (a), the chemical shift of the ^{15}N-labeled amino acids is highlighted by vertical lines and the chemical shifts of other amino acids by horizontal lines. Resonances relevant to the register determination are highlighted by colored circles in (a) and colored arrows in (b).

dx.doi.org/10.1021/ja111239r |*J. Am. Chem. Soc.* 2011, 133, 5432–5443

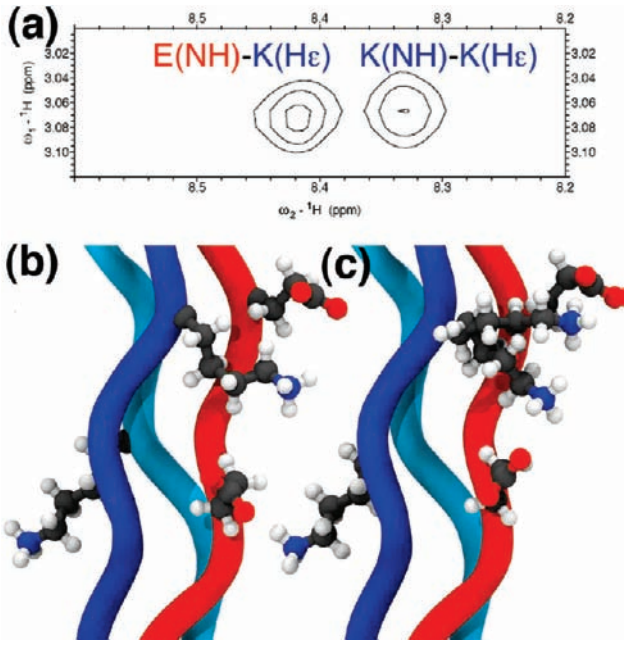

Figure 6. (a) ^{1}H,^{1}H-NOESY spectrum and (b,c) molecular models highlighting the interaction between charged residues in WG(PKGPOG)$_5$·WG(EOG)$_{10}$·WG(PKGPOG)$_5$. The model in (b) satisfies conformational constraints from (a) but prevents the formation of salt bridges and is depicted as the average between two possible hydrogen-bonded conformations in (c).

showing that the charge pair interactions between different chains are not equivalent and the K−E charge pair is most stable between the middle and lagging chains.[24]

The NOESY spectrum of this system also allows the study of the interaction between oppositely charged amino acids, which we rationalize as the driving force behind the self-assembly process. Of particular interest are the cross-peaks between the lysine ε-protons and both the lysine and the glutamate amide protons (Figure 6a). In previous studies, we have identified a cross-peak between the last methylene group of the basic side chain and the amide proton of the acidic residue located in the adjacent strand, two amino acids down in sequence.[10] This resonance arises because of the extended conformation of the positively charged residue, which is adopted to interact efficiently with the negatively charged residue. Another peak, that is barely observable in a previously published ABC heterotrimer but is strong in this collagen assembly, arises between the same methylene group and its own amide proton. Such a cross-peak is barely noticeable in the ABC system with a ratio between the interstrand and intraresidue NOEs of 5. In the case of WG(PKGPOG)$_5$·WG(EOG)$_{10}$· WG(PKGPOG)$_5$, the ratio between these two peaks decreases to 0.85, indicating that the distance between the lysine ε-methylene and its own amide proton is about the same as the distance to the acidic residue on the opposite strand. Figure 6b shows a model of the charged residue's side chain conformation for this system satisfying constraints derived from the NMR data. In this conformation, the amino group in the lysine residue is not able to effectively interact with either of the carboxylates of the negative chain. We attribute the observed resonances to a dynamic equilibrium of two possible charge paired states between lysine and the two successive glutamates (Figure 6c). Such a frustrated interaction can be used to rationalize the low thermal stability of these systems (as compared to previously published electrostatically driven heterotrimers containing stable hydrogen-bonding interactions) and the fact that there is a lack of control over the register of the peptides.

2WG(PKGPOG)$_5$·WG(DOG)$_{10}$. As in the previous system, there is still serious overlap in the amide−glycine alpha region of the NOESY spectrum of this system. For this reason, and as mentioned in the previous discussion, the register for this system was determined using the amide−amide cross-peaks presented in the edited NOESY spectrum. The edited NOESY spectrum for this system (Figure 7a) shows a cross-peak pattern similar to the one observed for WG(PKGPOG)$_5$·WG(EOG)$_{10}$·WG(PKGPOG)$_5$ (Figure 5a). Once again, the chemical shifts of the labeled amino acids are marked by vertical lines, while the glycines that they interact with are marked by horizontal lines. The register of the triple helix can be determined in a similar manner following the same naming convention. If we start considering G$_{O1}$, two NOEs can be observed: one going to the glycine in the second triplet of the DOGDOG repeat, labeled as G$_{D2}$, and one going to the PKG triplet in the second positive chain, G$_{K2}$. G$_{O2}$ also shows a cross peak to G$_{D2}$, proving that this system also chooses an ABA arrangement with the register being WG(PKGPOG)$_5$·WG(DOG)$_{10}$·WG(PKGPOG)$_5$, because other registers would require a cross-peak between the two labeled amino acids. Figure 7b and c shows a sequence repeat to clarify the naming conventions used in the discussion and a model of the heterotrimeric triple helix. Furthermore, the observed NOEs between the glycine amide protons are highlighted in Figure 7c using colored arrows that match them to colored circles in Figure 7a. As in the previous case, not enough resonances are observed to fully determine the minor register, but the presence of the cross-peak between both POG glycines suggests the WG(PKGPOG)$_5$·WG(PKGPOG)$_5$·WG(DOG)$_{10}$ register, similar to the previous system.

The interaction between the charged residues can also be studied using the NOESY spectrum of this system. As in the previously discussed heterotrimer, cross-peaks between the lysine ε-protons and the lysine and glutamate amide protons are present (Figure 8a). The ratio between the interstrand and intraresidue NOEs is 1.5 for this system, as compared to 5 in our ABC heterotrimer directed by lysine−glutamate charge pairs, indicating a different conformation of the side chains. In Figure 8b, a model of the charged residue's side chain conformation for this system satisfying constraints derived from the NMR data is depicted. This conformation prevents an effective interaction between the oppositely charged moieties, and thus we attribute the observed resonances to a dynamic equilibrium of two possible charge paired states between lysine and the two successive aspartates (Figure 8c). Therefore, the charge−pair interactions present in this system are more similar to the AAB system discussed in the previous section, in which the negatively charged amino acid corresponds to glutamic acid, than to our previously studied ABC system driven by K−D ionic hydrogen bonds. It should be noted that our previously published ABC heterotrimer containing lysine−aspartate charge pairs does not exhibit compositional control, as a homotrimer is formed by one of the peptides, but it does produce a single register heterotrimer.

dx.doi.org/10.1021/ja111239r |*J. Am. Chem. Soc.* 2011, 133, 5432–5443

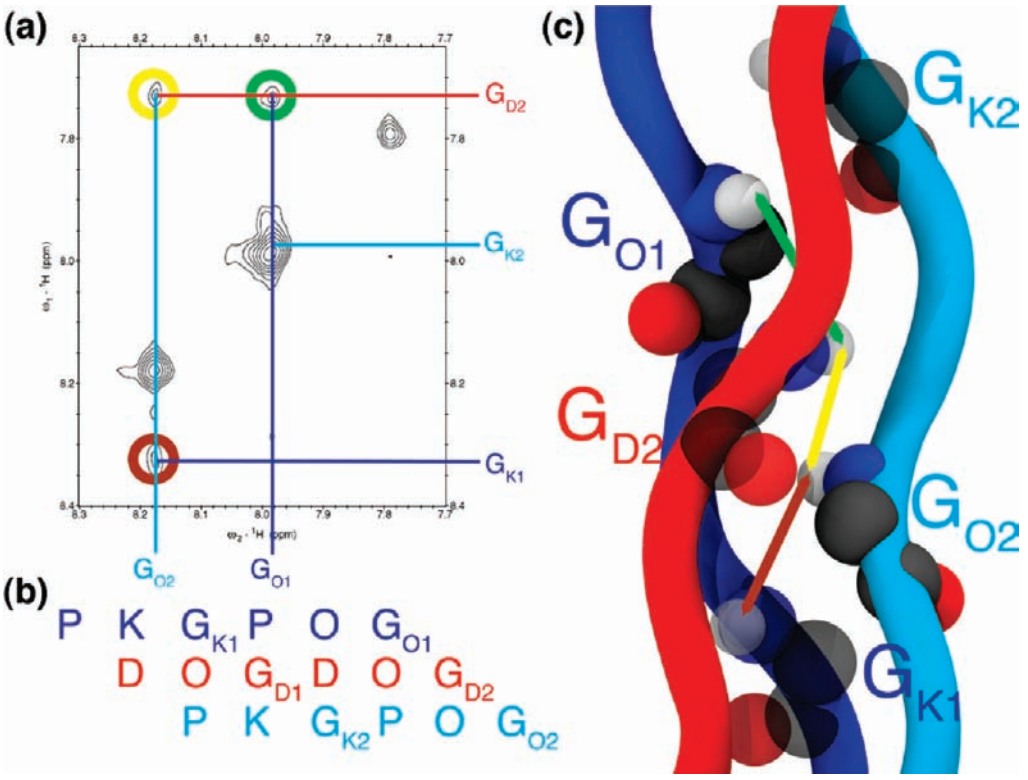

Figure 7. (a) ^{1}H,^{1}H-edited NOESY spectrum, (b) molecular model highlighting the glycine packing interactions at the core of the helix, and (c) sextet repeat of WG(PKGPOG)$_5$·WG(DOG)$_{10}$·WG(PKGPOG)$_5$. In (a), the chemical shift of the ^{15}N-labeled amino acids is highlighted by vertical lines and the chemical shifts of other amino acids by horizontal lines. Resonances relevant to the register determination are highlighted by colored circles in (a) and colored arrows in (b).

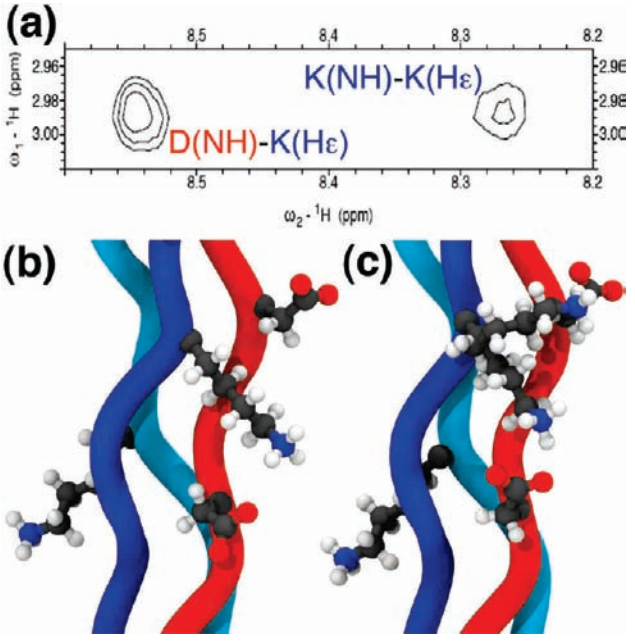

Figure 8. (a) ^{1}H,^{1}H-NOESY spectrum and (b,c) molecular models highlighting the interaction between charged residues in WG(PKGPOG)$_5$·WG(DOG)$_{10}$·WG(PKGPOG)$_5$. The model in (b) satisfies conformational constraints from (a) but prevents the formation of salt bridges and is depicted as the average between two possible hydrogen-bonded conformations in (c).

CONCLUSIONS

In this Article, we examine triple helices with R—D-, R—E-, K—D-, and K—E-based salt bridges. The heterotrimers utilize both positive and negative design in which desired heterotrimers are reinforced by favorable interactions of oppositely charged amino acids while undesirable homotrimers are minimized by reducing the use of stabilizing POG triplets in addition to incorporating charge repulsion. Two triple helices (PKGPOG)$_5$·(EOG)$_{10}$·(PKGPOG)$_5$ and (PKGPOG)$_5$·(DOG)$_{10}$·(PKGPOG)$_5$ are the first reported high-stability collagen-like heterotrimers to form, while none of the potential peptides form homotrimers, demonstrating the success of the negative design aspect of this method. 2D solution NMR results on these peptide systems demonstrate that, for the first time, a heterotrimeric system is reported in which there is control over heterotrimer composition such that all species within the system are of a single composition. In contrast, all previous reports on POG-containing heterotrimeric systems utilized peptides that formed homotrimers of various quantities. Furthermore, all systems containing the combination of lysine and aspartic acid, regardless of the charge distribution, formed heterotrimers. This suggests the possibility of a direct interaction between the charged residues similar to previous reports on an ABC heterotrimer and a special role for these types of interactions in collagen stabilization.[10] We observe that the arginine—aspartic acid charge pair cannot form a heterotrimer in any of the tested systems and believe that this is due to the interaction between the arginine side chain with a backbone carbonyl, which prevents the arginine from adopting the conformation necessary to optimally

dx.doi.org/10.1021/ja111239r |J. Am. Chem. Soc. 2011, 133, 5432–5443

hydrogen bond with aspartic acid. Finally, the composition and ionic strength of examined buffer systems were found to play a large role in determining heterotrimer stability in systems where homotrimers were also present. Together, our results provide a novel design scheme for synthetic extracellular matrix mimetics as well as a better understanding of the self-assembly of collagenous sequences.

■ ASSOCIATED CONTENT

Supporting Information. MALDI-MS and ESI-MS data, HPLC purification, NMR processing, and additional CD analysis for all peptides and peptide mixtures. This material is available free of charge via the Internet at http://pubs.acs.org.

■ AUTHOR INFORMATION

Corresponding Author
jdh@rice.edu

■ ACKNOWLEDGMENT

This work was funded in part by NSF CAREER Award (DMR-0645474), the Robert A. Welch Foundation (Grant No. C1557), the Camille Dreyfus Teacher Scholar Awards Program, and the Norman Hackerman Advanced Research Program.

■ REFERENCES

(1) Di Lullo, G. A.; Sweeney, S. M.; Korkko, J.; Ala-Kokko, L.; San, A., J. D. *J. Biol. Chem.* **2002**, *277*, 4223–4231.

(2) Heino, J. *BioEssays* **2007**, *29*, 1001–1010. Kadler, K. E.; Baldock, C.; Bella, J.; Boot-Handford, R. P. *J. Cell Sci.* **2007**, *120*, 1955–1958. Baronas-Lowell, D.; Lauer-Fields, J. L.; Fields, G. B. *J. Liq. Chromatogr. Relat. Technol.* **2003**, *26*, 2225–2254. Brodsky, B.; Persikov, A. V. *Adv. Protein Chem.* **2005**, *70*, 301–339. Shoulders, M. D.; Raines, R. T. *Annu. Rev. Biochem.* **2009**, *78*, 929–958.

(3) Shah, N. K.; Ramshaw, J. A.; Kirkpatrick, A.; Shah, C.; Brodsky, B. *Biochemistry* **1996**, *35*, 10262–10268.

(4) Xu, Y.; Bhate, M.; Brodsky, B. *Biochemistry* **2002**, *41*, 8143–8151.

(5) Persikov, A. V.; Ramshaw, J. A.; Brodsky, B. *J. Biol. Chem.* **2005**, *280*, 19343–19349.

(6) Persikov, A. V.; Ramshaw, J. A.; Kirkpatrick, A.; Brodsky, B. *Biochemistry* **2000**, *39*, 14960–14967.

(7) Okuyama, K.; Arnott, S.; Takajagani, M.; Kakudo, M. *J. Mol. Biol.* **1981**, *152*, 427–443. Okuyama, K.; Wu, G.; Jiravanichanun, N.; Hongo, C.; Noguchi, K. *Biopolymers* **2006**, *84*, 421–432.

(8) Bella, J.; Eaton, M.; Brodsky, B.; Berman, H. M. *Science* **1994**, *266*, 75–81. Kramer, R. Z.; Bella, J.; Brodsky, B.; Berman, H. M. *J. Mol. Biol.* **2001**, *311*, 131–147. Xu, Y.; Hyde, T.; Wang, X.; Bhate, M.; Brodsky, B.; Baum, J. *Biochemistry* **2003**, *42*, 8696–8703. Bretscher, L. E.; Jenkins, C. L.; Taylor, K. M.; DeRider, M. L.; Raines, R. T. *J. Am. Chem. Soc.* **2001**, *123*, 777–778. Eberhardt, E. S.; Panasik, N.; Raines, R. T. *J. Am. Chem. Soc.* **1996**, *118*, 12261–12266. Holmgren, S. K.; Bretscher, L. E.; Taylor, K. M.; Raines, R. T. *Chem. Biol.* **1999**, *6*, 63–70. Holmgren, S. K.; Taylor, K. M.; Bretscher, L. E.; Raines, R. T. *Nature* **1998**, *392*, 666–667.

(9) Madhan, B.; Xiao, J.; Thiagarajan, G.; Baum, J.; Brodsky, B. *J. Am. Chem. Soc.* **2008**, *130*, 13520–13521.

(10) Fallas, J. A.; Gauba, V.; Hartgerink, J. D. *J. Biol. Chem.* **2009**, *284*, 26851–26859.

(11) Gauba, V.; Hartgerink, J. D. *J. Am. Chem. Soc.* **2007**, *129*, 2683–2690.

(12) Gauba, V.; Hartgerink, J. D. *J. Am. Chem. Soc.* **2007**, *129*, 15034–15041.

(13) Gauba, V.; Hartgerink, J. D. *J. Am. Chem. Soc.* **2008**, *130*, 7509–7515. Venugopal, M. G.; Ramshaw, J. A.; Braswell, E.; Zhu, D.; Brodsky, B. *Biochemistry* **1994**, *33*, 7948–7956.

(14) Persikov, A. V.; Ramshaw, J. A. M.; Kirkpatrick, A.; Brodsky, B. *Biochemistry* **2005**, *44*, 1414–1422.

(15) Kar, K.; Ibrar, S.; Nanda, V.; Getz, T. M.; Kunapuli, S. P.; Brodsky, B. *Biochemistry* **2009**, *48*, 7959–7968.

(16) Krishna, O. D.; Kiick, K. L. *Biomacromolecules* **2009**, *10*, 2626–2631. Mechling, D. E.; Bachinger, H. P. *J. Biol. Chem.* **2000**, *275*, 14532–14536. Ottl, J.; Battistuta, R.; Pieper, M.; Tschesche, H.; Bode, W.; Kuhn, K.; Moroder, L. *FEBS Lett.* **1996**, *398*, 31–36.

(17) Byers, P. H. *Philos. Trans. R. Soc., B* **2001**, *356*, 151–157. Kelly, J. W.; Byers, P. H.; Helenius, A.; Swoboda, B. E. P. *Philos. Trans. R. Soc., B* **2001**, *356*, 157–158. Myllyharju, J.; Kivirikko, K. I. *Trends Genet.* **2004**, *20*, 33–43. Ricard-Blum, S.; Ruggiero, F.; van, d. R., M. *Top. Curr. Chem.* **2005**, *247*, 35–84.

(18) Russell, L. E.; Fallas, J. A.; Hartgerink, J. D. *J. Am. Chem. Soc.* **2010**, *132*, 3242–3243.

(19) Li, Y.; Mo, X. A.; Kim, D.; Yu, S. M. *Biopolymers* **2011**, *95*, 94–104.

(20) Xu, F.; Zhang, L.; Koder, R. L.; Nanda, V. *Biochemistry* **2010**, *49*, 2307–2316.

(21) Schanda, P.; Kupce, E.; Brutscher, B. *J. Biomol. NMR* **2005**, *33*, 199–211.

(22) Yang, W.; Chan, V. C.; Kirkpatrick, A.; Ramshaw, J. A. M.; Brodsky, B. *J. Biol. Chem.* **1997**, *272*, 28837–28840.

(23) Li, M.-H.; Fan, P.; Brodsky, B.; Baum, J. *Biochemistry* **1993**, *32*, 7377–7387.

(24) Gurry, T.; Nerenberg, P. S.; Stultz, C. M. *Biophys. J.* **2010**, *98*, 2634–2643.